High Throughput Simulation On The Impurity-Vacancy Diffusion Mechanism Using First-Principles Calculations.

Ignacio Martin-Bragado
Synopsys Inc.
Mountain View, CA, USA
nacho@synopsys.com

Yumi Park
Synopsys Inc.
Mountain View, CA, USA
yumip@synopsys.com

Christoph Zechner
Synopsys GmbH
Aschheim, Germany
zechner@synopsys.com

Yong-Seog Oh
Synopsys Inc.
Mountain View, CA, USA
yso@synopsys.com

***Abstract*—First principle calculations are a convenient and cost effective procedure to obtain the properties of the new and optimized materials required to solve the challenges of the next generation of semiconductor devices. But, even with reliable tools, the computation of the vacancy intermediated impurity diffusion can be challenging, especially in alloys. This work shows an algorithm to automate the process of such calculation by implementing a methodology to compute ring mechanisms in generic materials. Results for semiconductor (namely, Ge diffusion in Si and As diffusion in a $Si_{0.5}Ge_{0.5}$ random alloy) and non-semiconductor materials (Al diffusion in TiN) are shown. The results stress both a) the importance of the ring mechanism in understanding the diffusivity of impurities in crystalline materials, and b) the need for automatic algorithms that deal with the complexity of sampling and generating consistent configurations for such calculations.**

Keywords—DFT, impurity diffusion, high throughput, ring mechanism, silicon, silicon-germanium, titanium nitride.

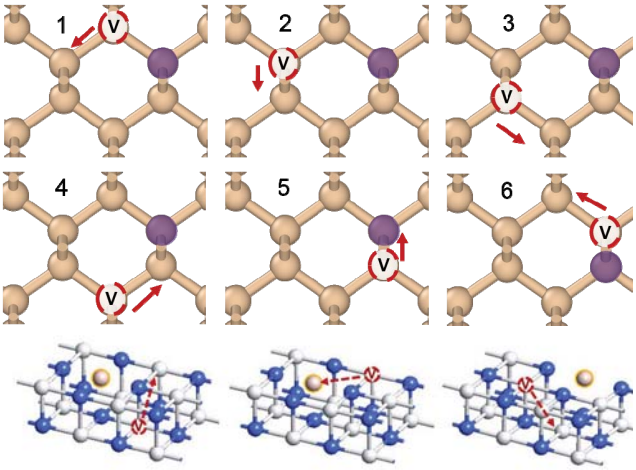

Figure 1 Ring vacancy mechanisms in Si (top) and TiN (bottom)

I. Introduction

The ever increasing demands for both new and old optimized materials to solve the challenges for the next generation of semiconductor devices require a constant research effort on the fundamental properties of well, and not that well known materials. Some of these fundamental properties are not feasible, or cost-effective, to be obtained experimentally, thus providing a big field of application for fundamental atomistic simulations. Of the many atomistic techniques, ab-initio, usually through a Density Functional Theory (DFT) implementation, is the most extended and promising today. But, even with reliable DFT tools, the computation of some simple physical properties can still be highly complicated in practice, mostly due to the multiple micro-configurations present in the material and a large number of calculations required for them. In this work we introduce an algorithm to decrease the source of human errors in those calculations, together with the possibility of incidentally introducing inconsistencies, while easing the use of DFT tools and increasing the productivity and reliability of them for TCAD use.

II. Model

In particular, we focus on the computation of impurity-vacancy diffusion in crystalline materials. For the impurity to escape a never ending pattern of swapping positions with the vacancy, a different mechanism is needed to represent the paths, where the vacancy comes back to the impurity from a different direction. Such mechanism, shown in Fig. 1 for Ge-V in Si and Al-V in TiN, is called ring mechanism, and it is responsible for the impurity-vacancy diffusion in crystals. The simulation of a ring mechanism involves the calculation of different trajectories for the vacancy to approach the impurity from a different side than the initial one. Since each intermediate step is repetitive they are suited for automating tasks of swapping the vacancy with the particle and performing the required NEB calculation. In the particular case where the host material is an alloy, the movement of the

vacancy through the ring might locally change the location of the alloy atoms, and this should be also taken into consideration. Thus, a generic algorithm to ensure the correct calculation of migration barriers would need to: 1) Sample the whole crystal for potential starting points for the impurity and vacancy. This is especially important for alloy materials, where the microscopic local configuration is not the same at different locations even if the host crystal is macroscopically homogeneous. 2) Compute the different trajectories in which the vacancy can come back to the impurity, then choose the shortest path. 3) For each sampling point and trajectory, build initial and final configurations then, proceed the geometry optimization of those configurations. 4) For each set of initial/final configurations, generate the initial path for NEB simulations then perform calculation to find minimum migration energy barrier in the path. And 5) Collect all the information, process it and provide the final results.

III. Solutions, Discussions

Using the above methodology, we have calculated the migration mechanisms for different materials using different impurities or dopants. We have focused our efforts in three cases. 1) A simple case for a substitutional Ge diffusing in pure Si paired with a V. 2) The diffusion of Al in a TiN crystal, showing how the algorithm is also applied to compound binary crystals. 3) The diffusion of As in a $Si_{0.5}Ge_{0.5}$ alloy.

A. GeV diffusion in silicon.

Fig. 2 shows the energetics of the ring mechanism for a Ge atom (schematically presented in Fig 1. top), paired with a V, diffusing in pure silicon using DFT first-principle calculations. Reaction coordinate represents the total distance between atomistic configurations. In Fig. 2 the reaction coordinates 0 Å, 9.5 Å, 11.5 Å correspond to a V at a lattice site in first nearest neighbor position of the Ge atom. In the Si diamond lattice, the vacancy needs to move away to the third nearest neighbor position of Ge (reaction coordinate 4.8 Å in Fig. 2) before it can return from a different direction. The figure also shows that the energy needed for Ge-V pair diffusion is made up by two contributions: First, the V needs to move away from

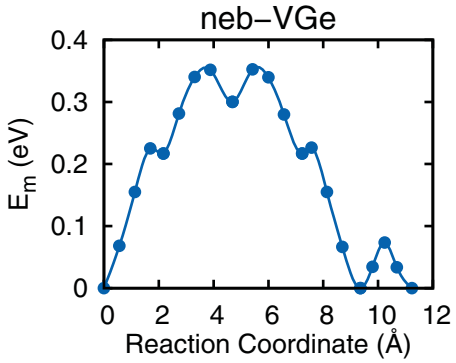

Figure 2 Ring mechanism for GeV in silicon

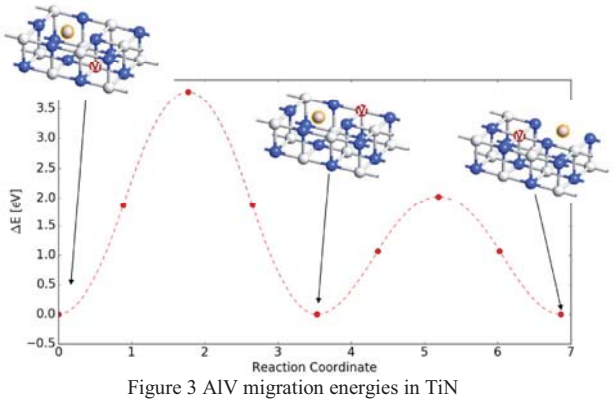

Figure 3 AlV migration energies in TiN

the most stable position, which is the first nearest neighbor position to the Ge atom. Then, to migrate from second to third nearest neighbor position, with similar energy, a migration barrier needs to be overcome. Besides, the small energy difference between second and third nearest neighbor position indicates that Ge-V pairs may easily dissociate, once the V reaches the third nearest neighbor position.

The Fig. 2 shows that the migration of the vacancy through the ring is the dominant mechanism, setting the barrier at 0.35 eV, while the exchange only accounts for a small energy contribution less than 0.1 eV. Also, the barrier is higher the farther the vacancy is from the initial position near the Ge, and both changes in the formation energy and migration energies account for it.

B. AlV diffusion in TiN.

A case where a compound binary crystal is used is shown in Fig. 3, which represents the migration energies of Al diffusing through the pairing with a Ti vacancy in TiN following the path shown in Fig. 1.

First, the algorithm, implemented in Sentaurus Materials Workbench [1] (SMW), automatically samples different paths and detects the minimum ring to consist of only three interchanges, as illustrated in Fig. 3.

The simulations, prepared along the description above, are run using a 64 atom TiN supercell, GGA PBE solid exchange correlation functional [2] and a basis set of Local Coupled Atomic Orbitals (LCAO). A 4x4x4 k-point Monkhorst Grid was used. The simulations are run using QuantumATK [3] driven by SMW.

The results show a total migration energy of 3.7eV. Interestingly, the barrier for the vacancy migration in the ring (3.7eV) is much higher than for the exchange (around 2.1eV), stressing the importance of including such intermediate configurations. Otherwise, the use of the exchange barrier as the main migration mechanism would have produced an underestimation of 1.6 eV.

A similar ring mechanism could be computed using empirical potentials showing that the methodology allows comparisons between different tools and techniques for the effortless selection of reliable simulations.

C. AsV diffusion in $Si_{0.5}Ge_{0.5}$.

Finally, the diffusion of substitutional arsenic intermediated by vacancies diffusion in a SiGe random alloy with 50% Ge atomic content has been performed using DFT calculations driven by SMW. The interest of these simulations underlies in two complexities introduced by the random alloy:

- First, even for a homogeneous macroscopic alloy sample, there are many different microscopic configurations: there is local inhomogeneity. Consequently, in contrast with the previous examples, the results depend on the particular position where a defect is introduced. Thus, a comprehensive study requires the repetition of the calculations by changing initial positions for the AsV defect. In other words, samples at different random positions in the 64 atom supercell are to be done.
- Second, as the vacancy traverses the system during the ring, if different constituents are found (i.e., Si vs. Ge) one has to take care of the memory of previous exchanges to properly place the Si and Ge. In other words, the local configuration changes as the vacancy follows the ring path, because not only the vacancy itself changes its position, but also the alloy atoms are moved during vacancy diffusion.

The former two points show the power of having automatic algorithms to perform consistent studies in alloys, because taking into account all possible configurations properly is almost impossible to do by hand or it would be at least very time consuming and error prone.

Fig. 4 shows several migration rings computed with the described methodology for the neutral AsV pair, using the QuantumATK DFT simulator driven by SMW. Several samplings have been taken and each sampling implies a ring

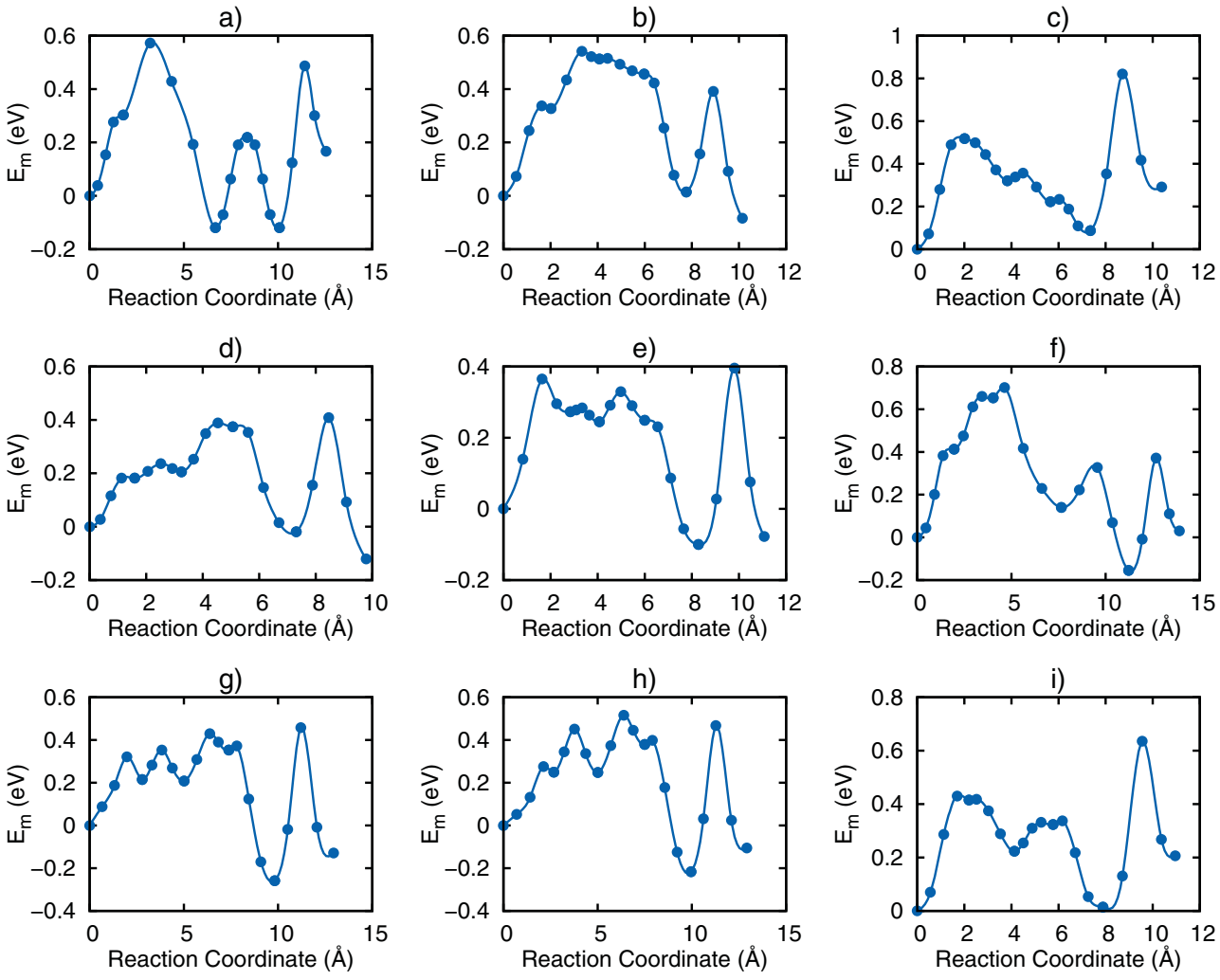

Figure 4 Ring mechanisms for the AsV migration in a SiGe alloy at different microscopic locations.

mechanism, with 5 segments computed with 1 NEB calculation each. Also, the NEBs require the creation and relaxation of the initial and final states, totaling 6 defect relaxations per ring. In contrast with non-alloy systems, the NEB segments cannot be shared between adjacent rings, because the history of each ring is important, as explained before. This means that for a modest sampling of 9 locations, one can expect 45 NEBs with a prerequisite of 90 defect relaxations. All these calculations (and the dependencies between them) are automatically generated and set up by SMW.

A 3x3x3 Monkhorst k-point sampling was used with the default QuantumATK basis set of LCAO and a GGA PBE solid exchange correlation functional [2]. A cut-off of 90 Hartree was used for integration in real space.

Fig. 4 clearly shows how different the results are depending on the particular sampling point, and also the lack of symmetry, especially when comparing any of the migration paths in Fig. 4 with the one in Fig. 2. The value of the maximum barrier for each path shows strong variations, being in the range of approximately 0.40 for Fig. 4 e) to 0.82 eV for c). Also, the position of the peak is not the same in all the rings, peaking at the 1st (a), the 2nd (b), the 3rd (d, f, h), and the 5th (c, e, g, i) segments, showing an obvious dependency with the location of particular Si and Ge atoms in the alloy microstructure. With some exceptions (f) the formation energy at the beginning and end of the ring is also different, and both changes in the migration and formation energies contribute to the total barrier of the migration paths. Finally, the relative contributions of the vacancy migrating in the ring vs. the last exchange are also not consistent. While in some paths (b, f) the migration contribution is clearly higher, in others (a, d, e, g, h) they are comparable while for the rest (c, i) the exchange accounts for the highest value.

It is worth noting that few single NEBs (for instance, 3rd and 4th segments in Fig. 4a) seem not to be starting or finishing in a local minimum, or at least metastable state. Although further investigation is needed to clarify why this is happening, probable solutions will include increasing the NEB number of images, currently at n=3, or the convergence criteria, set to 0.01 eV/Å in this work.

Finally, in some cases, although not shown here, it is also remarkable that some paths might contain less intermediate states than others. This happens when two adjacent NEBs collapse into the same, usually after one of the start or end defect configurations relaxed into an intermediate one (typically some split configuration).

What can be stated from Fig. 4 without hesitation is the importance of the ring mechanism, in particular of the vacancy migration part of it, to clearly picture the diffusivity mechanism of impurities coupled with such vacancies: the simple computation of swapping barriers is not enough, and in some cases might even be negligible.

The migration and formation energies collected from studies like the one represented in Fig. 4 could be used to feed Atomistic Kinetic Monte Carlo simulators to provide the macroscopic diffusivity in alloys of impurities intermediated by vacancies by simulating random walks which elementary hops use the calculated energies.

IV. Conclusions

In this work we have presented the methodology to study impurity-vacancy migrations in crystals. Results are presented for both semiconductor and non-semiconductor materials and also for alloy vs. non-alloy materials. In particular, for alloys, the complexities of producing enough paths to accurately sample the possible local configurations that impurities might find while diffusing coupled with vacancies, is shown and solved. Such solution involves the creation of algorithms that, without much user intervention, explore such configurations and issue the needed simulations for both the defects and the NEB of each of them. Finally, the physical importance of the ring mechanism in the overall diffusivity, in contrast with only considering the swapping of the impurity with the vacancy, is shown and discussed.

References

[1] Sentaurus Materials Workbench O-2018.06, Synopsys Inc.

[2] J. P. Perdew, A. Ruzsinszky, G. I. Csonka, O. A. Vydrov, G. E. Scuseria, L. A. Constantin, X. Zhou and K. Burke, Phys. Rev. Lett. 100, pp 136406, 2008

[3] QuantumATK O-2018.06, Synopsys Inc.

[4] J. Tersoff, Phys. Rev. B, 39, pp. 5566, 1989.